Available online at www.sciencedirect.com
SCIENCE DIRECT®
ELSEVIER
Nuclear Instruments and Methods in Physics Research B 234 (2005) 57–77
NIM B
Beam Interactions with Materials & Atoms
www.elsevier.com/locate/nimb

# Nanotubes for particle channeling, radiation and electron sources

S. Bellucci *

*INFN – Laboratori Nazionali di Frascati, P.O. Box 13, Via E. Fermi 40, 00044 Frascati, Italy*

Received 7 September 2004; received in revised form 11 January 2005
Available online 13 April 2005

**Abstract**

Carbon nanotubes consist in graphene sheets rolled into seamless hollow cylinders with diameters ranging from 1 nm to about 50 nm. They have been produced as both single walled and multiwalled nanotubes. The diameter of the MWNTs typically ranges from 10 to 50 nm, while the length exceeds 10 μm. For SWNTs, the diameter is only 1 nm and the length is up to 100 μm. Nanotubes exhibit unique physical and chemical properties as being a quasi-one dimensional material.

The main involvements of the INFN-LNF group in channeling researches are described, i.e. channeling of high energy beams in nanotubes (with the synthesis and characterization of the ordered nanotube samples), crystal extraction and collimation at IHEP (with the design and production of the bent crystals), crystal undulator R&D (with the characterization of the crystal undulator prototypes with SEM and the positron beam). We consider a precise determination of the optimal experimental conditions for channeling of accelerated particles (protons, positrons, photons, neutrons) through micro and nanostructured crystals and films of aligned nanotubes, as promising candidates for producing highly focused beams.


*PACS:* 81.07.De; 79.70.+q; 62.25.+g; 61.10.−i; 41.60.−m; 61.85.+p

*Keywords:* Carbon-nanotubes; Field-emission; Crystal-undulators; Radiation; Channeling; Positron-beams

## 1. Introduction

Carbon nanotubes are composed of graphene sheets rolled into seamless hollow cylinders with diameters ranging from 1 nm to about 50 nm. Several methods have been used to produce single walled as well as multiwalled nanotubes. The

* Corresponding author. Tel.: +39 06 9403 2888; fax: +39 06 9403 2427.
*E-mail address:* stefano.bellucci@lnf.infn.it

0168-583X/$ - see front matter © 2005 Elsevier B.V. All rights reserved.
doi:10.1016/j.nimb.2005.02.018

diameter of the MWNTs typically ranges from 10 to 50 nm, while the length exceeds 10 μm. For SWNTs, the diameter is only 1 nm and the length is up to 100 μm. In 1991, MWNTs were discovered in a carbonaceous stalagmite-like deposit by Iijima [1], which was left on an electrode after the recovery of fullerene soot produced by a carbon arc. SWNTs were discovered in 1993 during the course of synthesizing carbon nanocapsules filled with magnetic fine metal particles (Fe, Co, Ni) [2,3]. Since, then, a lot of research has been carried out on this novel carbon nanomaterial with much success. Nanotubes exhibit unique physical and chemical properties as being a quasi-one dimensional material. These nanotubes especially for SWNTs are either metallic or semimetallic, depending on the geometry of a graphene sheet rolled up into a tube (diameter and chiral angle) [4–6]. Nanotubes present one-dimensional confinement effects and behave as coherent quantum wires [7–10]. Mechanically nanotubes have high perfection in their structures and have the highest modulus of all known materials [11]. Due to these extreme properties, nanotubes are under investigation towards several applications, including electron field emitters [12], probes of scanning-type microscopes [13], hydrogen storage materials [14], electrode materials of secondary batteries and capacitors [15]. Among these proposed applications, field emission electron sources would be industrially the most promising and are nearly within reach of practical use.

Field emission involves the extraction of electrons from a solid by tunneling through the surface potential barrier. The emitted current depends directly on the local electric field at the emitting surface and on its work function. Field emission is important in several areas of industry, including lighting and displays. The relatively low voltages needed for field emission in nanotubes could be an advantage in many applications. The small diameter of carbon nanotubes is very favorable for field emission, the process by which a device emits electrons when an electric field or voltage is applied to it. The field has to be very high. When a high electric field is applied on a solid surface with a negative electrical potential, electrons from the solid are emitted into vacuum by the quantum mechanical tunneling effect. Such an extremely high field can be obtained on a sharp tip of very thin needle, because electric fields concentrate at the sharp points. The carbon nanotubes possess high aspect ratio, a sharp tip, high chemical stability and high mechanical strength, which make them good candidates for field emitters. In 1995, field emission from an isolated single MWNT was first reported by Rinzler et al. [16], and field emission from a MWNT film was reported by De Heer et al. [17]. Subsequently many studies on field emission from MWNTs [18–20] and SWNTs [21,22] were reported.

Significant progress in carbon-based electronics may come from employing irradiation, together with high-temperature annealing, in order to join CNTs together. In the future, doping CNTs with impurities introduced by ion irradiation could allow to control electronic properties of CNTs. Another important use of irradiation with energetic particles is given by their role in producing defects aimed at enhancing the chemical reactivity of CNTs, in order to engineer their properties.

Among the possible application of CNTs, the channeling of particle beams has been suggested in [23]. In principle, both straight and bent CNTs can effectively be used for high-energy (>1 GeV) proton channeling, provided the technological challenge of achieving an almost perfect alignment of CNTs with respect to the beam direction could be tackled effectively in the synthesis of samples.

## 2. Past experimental research activity

The carbon nanotubes are synthesized by the DC arc plasma, struck between two graphite rods. This type of synthesis yields high quantity of CNTs. We are also making progress in setting up a thermal CVD system of CNT synthesis. This set-up is greatly useful in synthesizing CNTs on a patterned surface (substrate). We have been successful in synthesizing both SW and MW CNTs under varying synthesis conditions. The synthesis parameters like plasma current, thermal gradients, etc. were varied for different experiments and the resulting samples studied with electron microscopy to determine the optimal conditions for CNT

synthesis. Also the samples from various parts of the synthesis chamber plus the cathode deposit were analyzed to establish the zone of maximum yield of nanotubes (in relation to the nanoparticles and so on).

The characterization of the samples was done with various electron microscopies for morphology determination as well as to study its electrical and field emitting properties. The main techniques employed for this study were:

(i) scanning electron microscopy (in house);
(ii) transmission electron microscopy;
(iii) Raman Spectroscopy;
(iv) field emission microscopy (in house);
(v) atomic force microscopy;
(vi) scanning tunneling microscopy.

Also some preliminary tests were done to study the electrical properties of individual nanotubes of other materials.

(i) The morphological analysis of our samples by SEM, TEM, STM and AFM indicate clearly the ratio and dimensions of the CNTs synthesized with our setup. In particular, SEM images of the CNT show that the ratio of nanotubes is very high (to an extent of more than 70%). The single walled nanotube were found to be having an average diameter of 1.3 nm and a length of a few microns. These single walled NT are also seen to exist in bundles of 20–40 nm. On the other hand, the multiwalled nanotubes have a wide range of diameter (from 20 to 60 nm), probably also existing in bundles of fibres.
(ii) The synthesized nanotubes were also studied under AFM. This was carried out to reconfirm the morphology of the nanotubes as well as to study the nanotube–substrate interactions. Three sets of nanotubes from the same sample were deposited on three different substrates, mainly HOPG (highly oriented pyrolytic graphite), silicon and mica and their atomic force spectroscopy studied. Substantial qualitative differences in the horizontal and vertical directions of the dimension were observed for nanotubes placed on different substrates. These differences clearly indicated the strong/weak interaction between the nanotube walls and the substrate's surface depending primarily on the substrate itself. Quantification of these results are in progress. This study will help in choosing appropriate substrates for specific applications. Preliminary results show that the adhesion of CNTs to HOPG is greatest – of the order of 6 times – as compared to its adhesion on mica or silicon. The lateral compression of the nanotube at HOPG indicates a strong interaction and hence a strong adhesion to the substrate. The lateral elongation of the nanotube on mica and silicon show a weak interaction with the substrate (consequently a strong interaction with the tip) and therefore a low adhesion coefficient.
(iii) The field emission properties of the samples were recorded (see next section below). Current stability experiments are also in progress to establish the reliability and durability (in terms of constant electron emission) of the CNTs.

Our experimental activity can be summarized as follows [24–31]:

- Manufacture of aligned and patterned carbon single walled nanotubes (SWNT) (ropes and isolated) and multiwalled nanotubes (MWNT) by arc discharge and thermal chemical vapour deposition (CVD).
- Purification and functionalization (for enhanced and selective purification) of the samples by chemical and physical treatments, including thermal oxidation and ultrasound sonication (collaboration with Burnham Institute, Univ. Perugia, CSM).
- Characterization of the samples by electron microscopies, i.e. SEM (CNR-IFN), STM (Univ. Roma Tor Vergata), AFM (IMM-CSIC, Univ. Roma Tre), TEM (Univ. Modena and Univ. Pune) and characterization of alignment of nanotube films by channeling of accelerated particle beams (IHEP-Protvino for protons and positrons, ILL-Grenoble for neutrons).

- Use of C nanotube films for the study of field emission properties and determination of their efficiency for the realization of vacuum gauges and electron emitters (collaboration with VARIAN).
- Analysis of the effect of nanotube alignment and patterning on the emission efficiency of the sample.
- Study of the emitted current in terms of spatial mapping.
- Study of the application for the manufacture of KV X-ray sources and gas discharge tubes based on C nanotubes (collaboration with HITESYS).
- Use of ordered C nanotube films for applications of the channeling mechanism to steering of accelerated particle beams.
- Manufacture of crystalline undulators (CU) based on micromachining of Si strips.
- Optimization of CU for the production of photons in the range 10–1000 keV.
- Realization of channeling structures inside graphite samples, by making use of a novel technique of nanofabrication using electron beams in collaboration with Hitesys R&D e Ambiente (Aprilia).
- Optimization of the channeling properties of the produced samples, in order to achieve alignment of the tubes at the level of a few mrad, i.e. ideal for accelerated particle beam steering, according to the Monte Carlo simulations.
- Determination of the configuration of the feasible CU to be used in concrete experiments the Frascati Beam Test facility (BTF) and the scheme of the experiment, based on simulation results.
- Synthesis and characterization of patterned films of aligned C nanotubes, comparing results obtained by different deposition methods.
- Study of the interaction of nanotubes with the AFM tip and different types of substrates.
- Optimization of the field emission properties of the arc-discharge and CVD produced nanotube thin-film samples, in order to achieve an efficient emission with high density of the emitted current, in collaboration with VARIAN (Torino) for applications to new kinds of sensor devices, e.g. pressure sensors.
- The study of new geometries in the cathode and the influence of the nanotube alignment will be pursued, in order to get maximal values of the emitted current.
- Also, for a large enough distance of the collector from the emitter (i.e. 5 cm for nanotubes having a diameter of about 30 nm) it will be possible to observe and study the kinetics of nanotubes at the very moment when the voltage is applied to the sample.
- Study of the anisotropy of the emitted current between the tube edges and their surfaces.

## 3. Relevant results achieved

We synthesized good quality samples of aligned ropes of SWNT, with the average tube diameter of 1.3 nm and a bundle diameter of 20–40 nm, as well as MWNT with diameter of 20–60 nm; we obtained a high yield in terms of C nanotube density in the sample (above 70%).

The electron microscopy characterization for a typical sample we produced by arc discharge is seen in Fig. 1 (collaboration CNR-IFN). The result of another deposition by arc discharge, obtained using a different experimental setup, is shown in Fig. 2. It looks very promising for a higher yield in nanotubes and a higher purity of the sample. The SEM characterization is however not sufficient to establish the very nature of such nanostructures, i.e. it is impossible to say only on the basis of SEM observations whether the tubular structures are empty or full, hence distinguishing C nanotubes from nanofibres. Thus, we proceed to a TEM analysis of the samples, with the result displayed in Fig. 3 (collaboration Univ. Pune) where a bundle of about 10 μm long SWNT without closures at their ends is shown on a scale of 1 μm. In Fig. 4 (left) we display a TEM image of a MWNT we manufactured, where the coaxial cylinders and the central channel in the tube are clearly seen. This image has been taken on a scale of 5 nm at the Univ. of Modena and shows clearly a structure closing one end of the nanotube. In this case one can estimate the diameter of such structure to be approximately 20 nm. Another TEM image of our samples is reported in Fig. 4 (right).

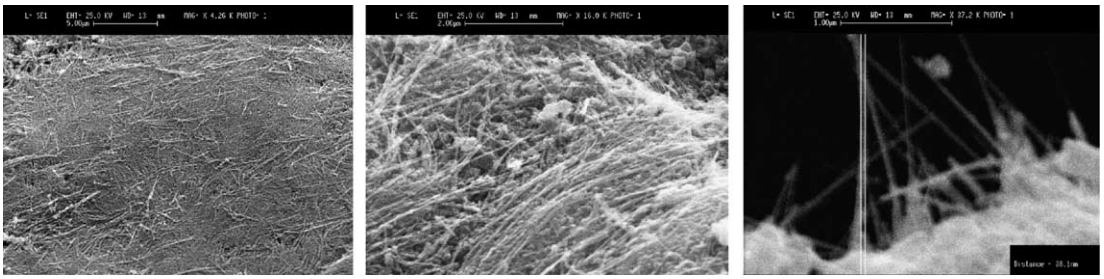

Fig. 1. SEM images of a cathodic deposit obtained at LNF by arc discharge.

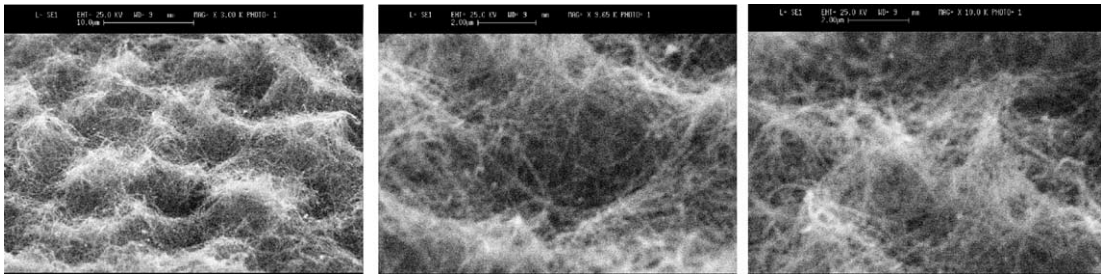

Fig. 2. SEM images of a nanotube carpet synthesized at INFN-LNF with a different arc-discharge setup, showing a very high ratio of nanotubes.

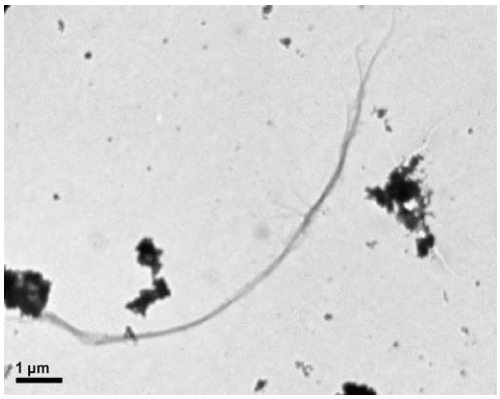


Fig. 3. TEM images of a carbon nanotube bundle obtained by arc discharge at INFN-LNF, shown on scales of 1 μm.

Using Raman spectroscopy (coll. CNR-ISMN Bologna) we investigated two different samples of carbon nanotubes produced by arc-discharge method: *31103 on screw* (as reported in Fig. 4, right) and *CD100A* (similar to Fig. 4, left). Let us recall that radial breathing modes (RBM), D and G lines are the most important lines in Raman spectra [32].

- The RBM Raman features (appearing between $120\ \mathrm{cm}^{-1} < \omega_{\mathrm{RBM}} < 250\ \mathrm{cm}^{-1}$ for SWNTs within $1\ \mathrm{nm} < dt < 2\ \mathrm{nm}$) correspond to the atomic vibration of the C atoms in the radial direction, as if the tube was breathing. In Fig. 5 we plot the Raman spectra of the samples *31103 on screw* and *CD100A*. Only the sample *CD100A* shows the presence of SWNT due to the energy peak position at about $200\ \mathrm{cm}^{-1}$.
- The Raman-allowed tangential mode in graphite is observed at $1582\ \mathrm{cm}^{-1}$, and is called the *G mode* (from graphite). The lineshape of the so-called G-feature is broadened for metallic SWNTs in comparison with the Lorentzian lineshape for semiconducting tubes, thus indicating the presence of free electrons in nanotubes with metallic character [33]. In Fig. 6 (left) the G line is divided in two peaks due the two different tangential atomic displacements of the tubes in the sample of Fig. 4 (left).

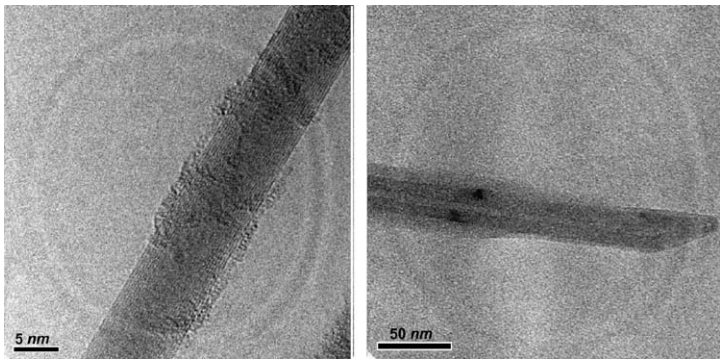


Fig. 4. TEM images of a MWNT obtained by the INFN-LNF group, shown on scales of 5 nm, 50 nm, respectively.

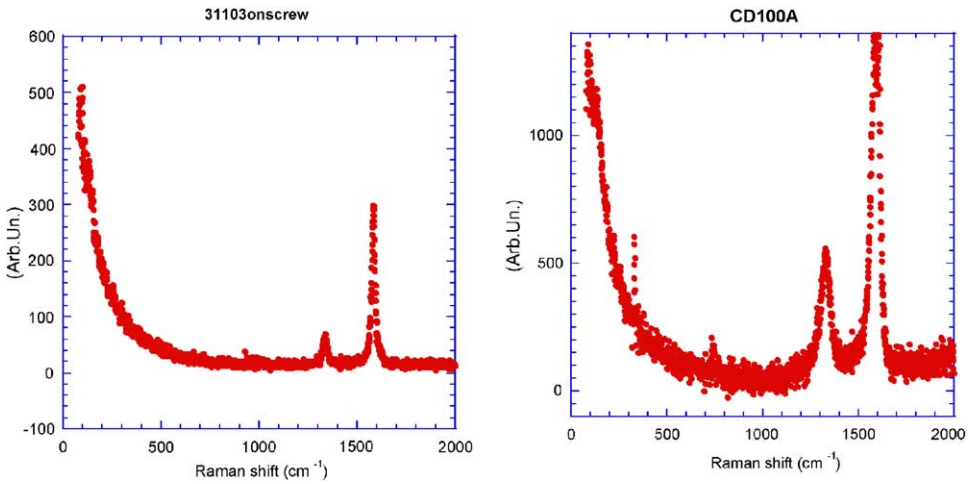


Fig. 5. Raman spectra of the samples 31103 on screw of Fig. 4 (right) and CD100A of Fig. 4 (left).

The broadening of the G line of the sample in Fig. 6 (right) shows the presence of metallic carbon nanotubes in the sample of Fig. 4 (right).

- It is possible to correlate the presence of the D-band with different defect types (such as heteroatoms, vacancies, heptagon–pentagon pairs, kinks or even the presence of impurities, etc.). The observation of large D-band peaks compared with the G peak intensity in SWNT bundles usually indicates the presence of amorphous carbon [34]. In both samples (see Fig. 6) the intensity of the D-band peaks is large showing the presence of amorphous carbon.

TEM images in Fig. 6 of the samples *31103 on screw* and CD100A, respectively, indicate the presence of MWNTs. For Raman scattering, MWNTs can be said to be an ensemble of carbon nanotubes with diameters ranging from small to very large. Because of the large diameter of the outer tubes for typical MWNTs, most of the characteristic differences that distinguish between the Raman spectra in carbon nanotubes from that for graphite are not so evident in MWNTs. The Raman features associated with the small diameter inner tubes can sometimes be observed when a good resonance condition is established [35], but it is not the usual result. The RBM from large diameter tubes is usually too weak to be observable. These properties make it more difficult to differentiate the Raman signal of MWNTs from that of graphite.

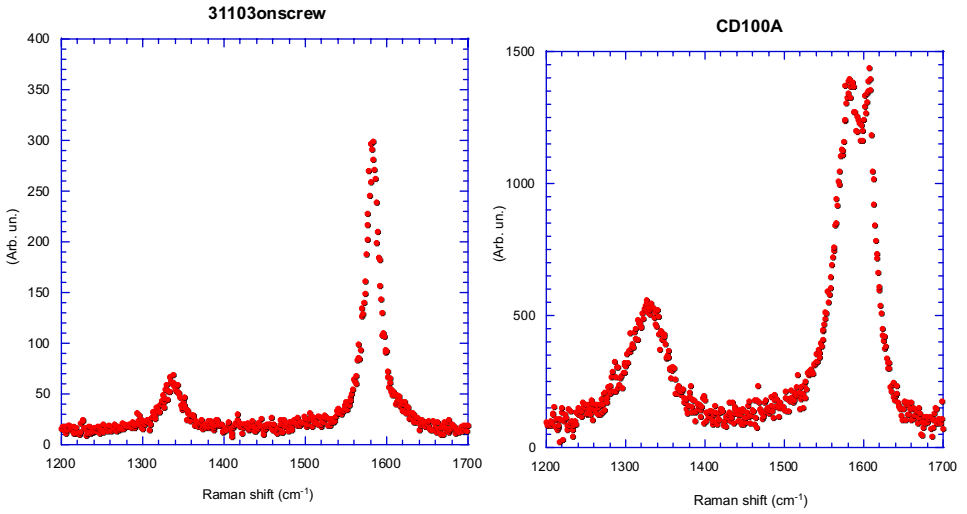


Fig. 6. D, G peaks in the Raman spectra of samples in Fig. 4.

Atomic force microscopy (AFM) studies of the carbon nanotubes that were synthesized by arc discharge have been carried out at IMM-CSIC, Madrid. The imaging was carried out to determine (a) the morphology and dimensions of the CNT and (b) to evaluate the friction coefficient of the nanotube with the substrate surface. Contact mode AFM was used for the imaging under a constant force. The images (see Fig. 7(a)) reconfirmed the dimensions of our nanotubes to be approximately 30–60 nm as detected from the SEM images earlier. The nanotube samples were initially dispersed in isopropyl alcohol and sonicated for a few hours. Drops of this were then suspended on three different substrates, namely HOPG, silicon wafer and mica sheet (Fig. 7(b)).

The adhesion of nanotubes was found to be highest for HOPG, as compared to Mica and silicon (where the nanotubes got displaced easily by the AFM tip). Also it was observed that the nanotubes got laterally compressed on a HOPG surface (Fig. 8) (due to Van der Waals interaction of the nanotubes with the substrate) to a ratio of 0.5. For mica and silicon there was lateral elongation of the order of nearly 3 times (Fig. 9), indicating that the interaction of the tube with tip was far greater than the interaction of the tube surface with substrate. The study of these results should be further continued and is quite interesting from the point of application-oriented studies of nanotubes. From such results we can say e.g. that mica and silicon can be used for nanomechanics and HOPG for applications where strong bonding of nanotubes to substrates is required, as it is the case for field emitting devices.

In Fig. 10 we show a STM characterization (coll. Univ. Roma Tor Vergata) of the CNT samples deposited by arc discharge in our group. The samples of the nanotubes were initially dispersed in isopropyl alcohol and sonicated for a few hours. Drops of this were then suspended on a HOPG substrate. The results shown in the figures confirm the morphological properties already described above, with the presence of SWNT which occur in bundles of aligned tubes tens of microns long, with an average tube diameter of 1–2 nm and a bundle diameter of 20–40 nm.

Good field emission properties of the samples, with activation fields of 0.4 V/μm and a typical current emission of order 10 m A/cm$^2$ (for a voltage of about 1 V/μm, see Fig. 10(c) Graph 1: *I–V* measurements). These results are competitive with the best results reported by Saito et al. [54]. We started to study the stability of the emitted current, which is a very important constraint for the proposed applications. Preliminary results are shown in Fig. 10 (c) Graph 2. We also repeated the measurements of the emitted current for samples (as

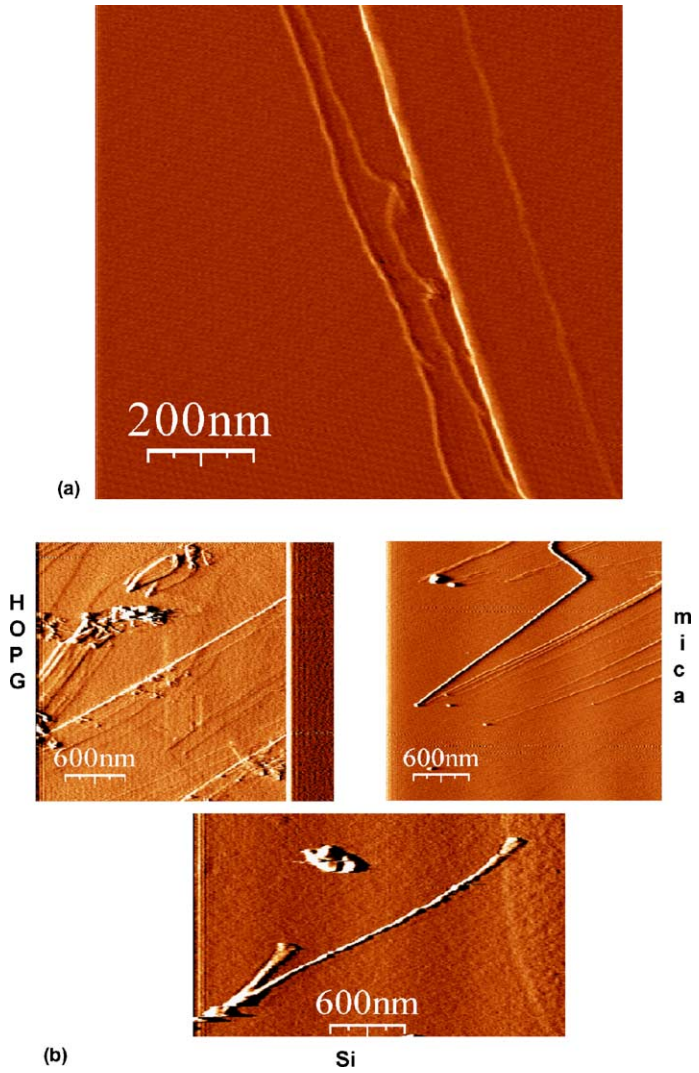


Fig. 7. (a) AFM image of CNT synthesized by arc discharge showing bundles of MWNT. (b) AFM images of CNT on (a) HOPG, (b) mica and (c) silicon surface.

seen in Fig. 4) obtained using different conditions. The data collected look very promising for a higher yield in nanotubes and a higher purity of the sample. The production of micro and nanostructured films, as promising candidates for producing X-ray sources and gas discharge tubes, has potential applications in radiotherapy, biology and space research. Our activity has a potential impact on the fields of vacuum technology and sensors, for biological and aerospace applications, as well as for electromedical devices based on innovative materials.

## 4. Research objectives of our crystal undulator project

We present next our recent experimental proof [36] for the feasibility of creation of a crystalline undulator (CU), review the scientific background

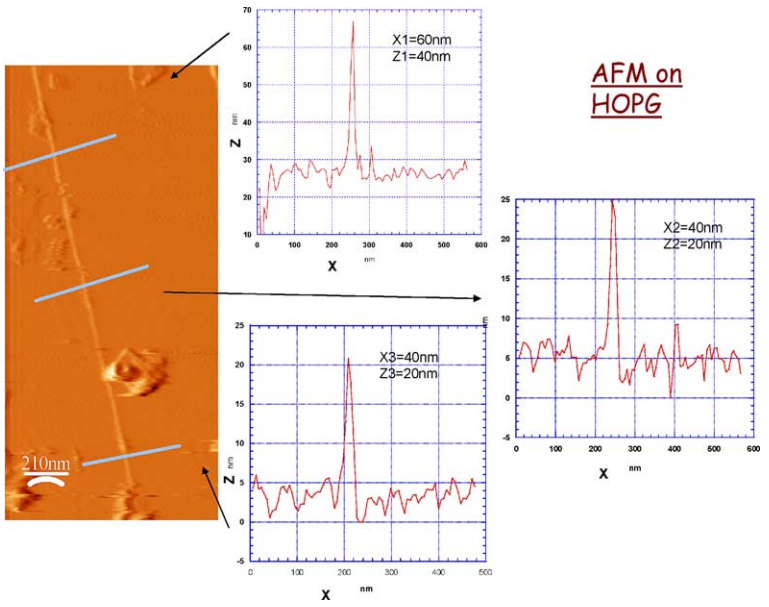


Fig. 8. AFM on HOPG shows a lateral compression ($Z < X$) of the nanotube (due to strong interaction between the substrate and the tube surface).

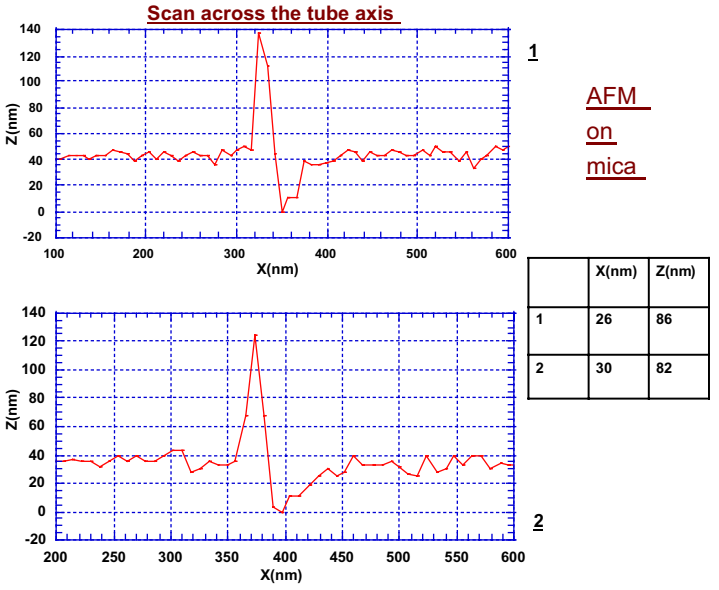


Fig. 9. AFM image shows a lateral elongation of the nanotube (due to strong interaction between the tip and the tube surface).

for CU and propose the world-first experimental study of photon emission in the field of periodically deformed crystallographic planes serving as an undulator.

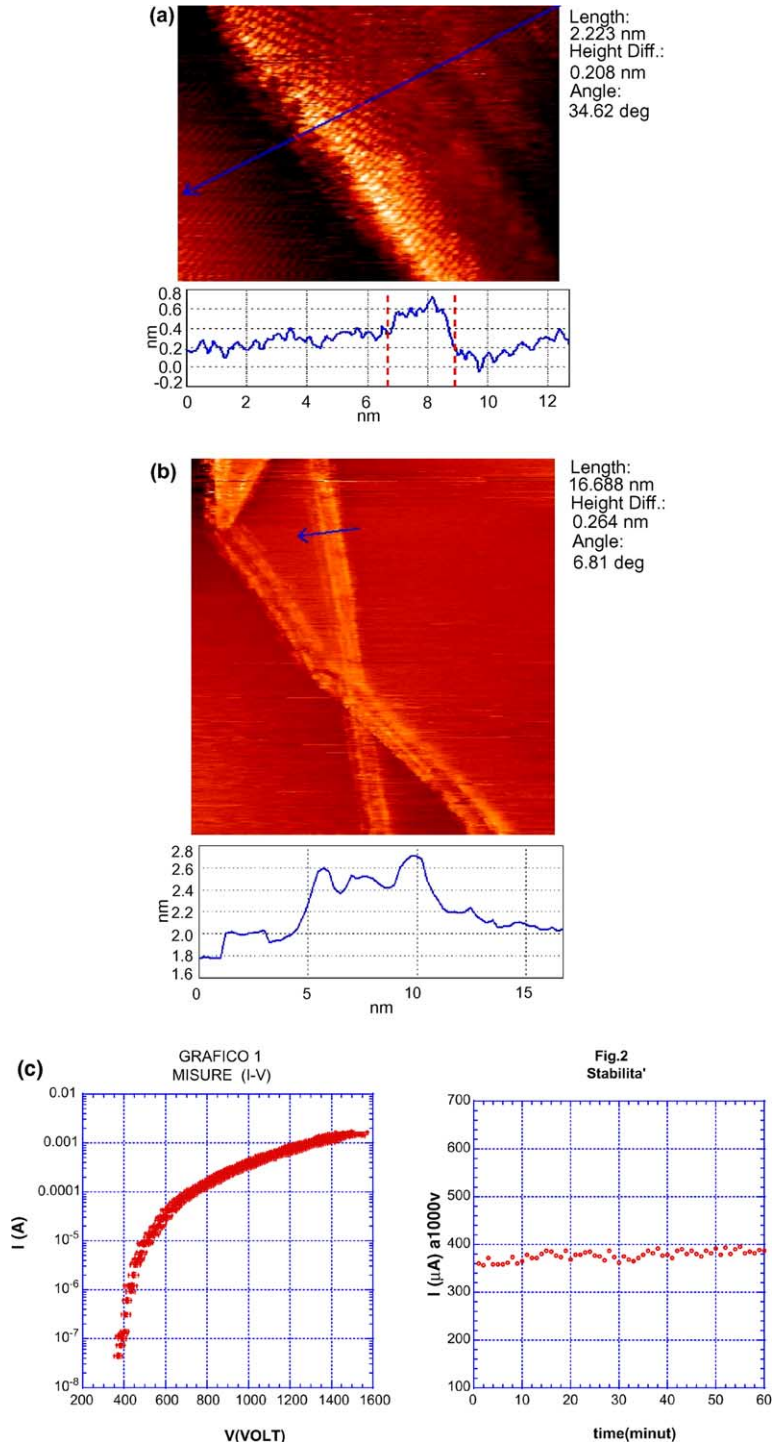


Fig. 10. (a) STM image of a SWNT on HOPG substrate. (b) STM image showing SWNT bundles crossing. (c) We analyzed the stability of the sample, collecting the emitted current for 1 h, for a constant value of the applied field 1000 V. In Graph 2 above (right) we report this measurement, yielding an average value (377 ± 17) μA.

The activities will be centered about two proposed accelerator experiments, one at LNF Frascati with 500–800 MeV positrons, and another one at IHEP Protvino with 2–10 GeV positrons. Within this project, we foresee the following research directions:

1. Detailed realistic simulations of particle channeling in crystal undulator aiming to optimize the undulator in general and for the conditions of the experiments at IHEP with positrons of 2–10 GeV and at LNF with positrons of 500–800 MeV. Prediction of the results of the experiments.
2. Design and manufacture of crystal undulators with different parameters (period, length, etc.) for the experiments at IHEP and at LNF.
3. Characterization of the undulators by means of X-rays and optical microscopy.
4. Channeling tests of the undulators in the beam of high-energy protons at IHEP.
5. Crystal undulator experiment (photon emission) at IHEP with positrons of 2–10 GeV.
6. Crystal undulator experiment (photon emission) at LNF with positrons 500–800 MeV.
7. Proof-of-principle experiment with high-energy protons and positrons on channeling in nanostructured material. Simulation of channeling physics in nanostructured material in order to verify the model against the experiments and to make a feasibility study for an undulator based on nanotube channeling.

The major objective of this research is the observation of undulator photons emitted with expected energy in a crystalline undulator, the measurement of the CU spectrum, the demonstration that the crystalline undulator works for the first time in the world.

The wavelength $\lambda$ of a photon emitted in an undulator is in proportion to the undulator period $L$ and in inverse proportion to the square of the particle Lorentz factor $\gamma$. The minimal period $L$ achieved presently with the electromagnetic undulators is limited to several millimeters, with respective restriction on the photon energy order of $\hbar\omega = 2\pi\hbar\gamma^2 c/L$. The crystalline undulators with periodically deformed crystallographic planes offer electromagnetic fields in the order of 1000 T and could provide a quite short period $L$ of an undulator in sub-millimeter range. This way one can arrange for substantial amplitudes $A$ of oscillation for the particles channeled through the undulator and thus increase the intensity of the radiation.

With a strong world-wide attention to novel sources of radiation, there has been broad theoretical interest to compact crystalline undulators, with some approaches covering also nanotechnology to make use of nanotubes to guide radiating particles [27,37–43]. Nanotubes with a length 50 μm, may produce a 5 mrad deflection in a parallel proton beam of 1 GeV [27]. Hence they may be applied to beam extraction at accelerators. Indeed, the beam bending effect in C nanotubes of 1 nm size is comparable to that of Si crystals.

Three different ideas have been discussed in the literature how to make a crystalline undulator. The historically first idea [37] suggested to apply ultrasonic waves for periodical deformation of crystal lattice. Another idea [43] proposed to use the graded composition strained layers in superlattices, in particular, in $Ge_xSi_{1-x}$ superlattices in which $x$, the concentration of Ge, varies periodically. The latest idea [44] discussed in the literature is to provoke periodical strains in the crystal by covering its surface by thin narrow periodically placed strips of $Ge_xSi_{1-x}$ grown on Si substrate. None of these ideas have been realized so far.

In bent crystal channeling experiments at IHEP Protvino with 70 GeV protons it was found that accidental microscratches on a crystal surface cause a deformation of crystallographic planes to substantial depths, down to a few hundred microns [45]. Therefore this effect can be used for creation of CU by making a periodic series of microtrenches on the crystal surface.

Recently, our collaboration has presented this idea and reported world first realization of a crystalline undulator [36]. One face of a silicon crystal was given periodic microscratches (grooves) by means of a diamond blade. The X-ray tests of the crystal deformation due to given periodic pattern of surface scratches have shown that a sinusoidal-like shape is observed on both the scratched surface and the opposite (unscratched) face of the crystal, that is, a periodic sinusoidal-like deformation goes

through the bulk of the crystal. This opens up the possibility for experiments with high-energy particles channeled in crystalline undulator, a novel compact source of radiation.

For the first experimental proof of the method, a special diamond blade scratched one face of a silicon plate with a set of parallel grooves. A sample with dimensions of $50 \times 17 \times 0.48\ \mathrm{mm}^3$ was prepared at the U. Ferrara and IHEP-Protvino in the Spring 2002 from a commercial silicon wafer. The large polished faces of the sample were parallel to crystal planes (0 0 1), other faces were parallel to planes (0 1 1) and (0 1 −1). On one of the large faces, 16 grooves were made with 1 mm period along the 50 mm edge. The grooves had 100 μm width and the same depth (see Fig. 11(a) for a schematic representation of the characteristics of the sample). In Fig. 11(b) a SEM image of a microgroove scratching the crystal surface is seen.

For another of our samples SEM images (see Fig. 12, coll. IFN-CNR) show 50 μm grooves on the undulator surface spaced by 200 μm obtained by micromachining at Protvino, what produces periodical deformations that propagate in the bulk of the crystal. The size of the grooves and the pressure of the scriber are found empirically, aiming at

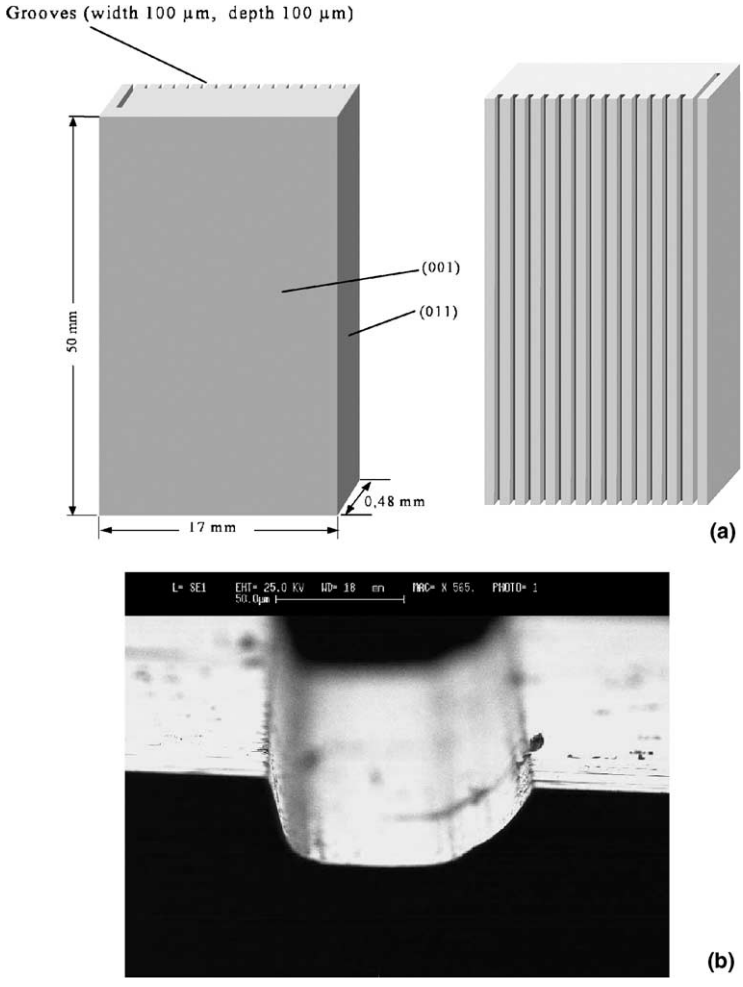


Fig. 11. (a) Schematic description of a sample prepared by U. Ferrara and IHEP-Protvino in Spring, 2002. (b) SEM image of a microgroove on the crystal surface.

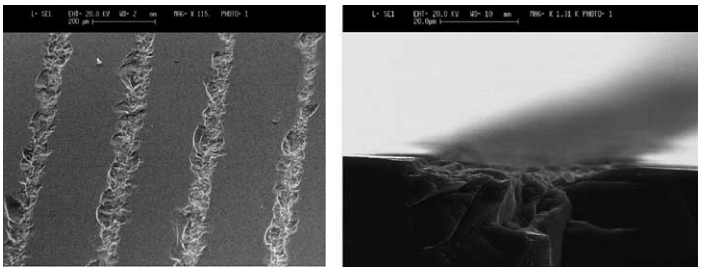

Fig. 12. SEM images of a Si CU showing 50 μm grooves spaced by 200 μm on the undulator surface obtained at IHEP-Protvino; the side view on the left shows how micromachining produces periodical deformations that propagate in the bulk of the crystal.

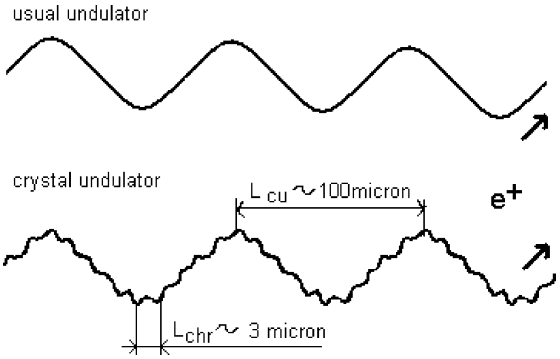


Fig. 13. Peculiarities of a crystalline undulator.

producing maximal deformations while the crystal is not breaking yet.

Particle trajectories in a deformed crystal are more complicated than in a usual undulator (see Fig. 13). Undulator radiation is accompanied by a harder component (channeling radiation) due to channeling with a smaller period of oscillations $L_{\mathrm{chr}} \sim 3$ μm (for typical energies of a few giga electron volts, where undulators are used). On the other hand the channeling component of particle motion in a CU has the amplitude of oscillations also small $A_{\mathrm{chr}} \sim 1$ Å.

The prepared sample was carefully investigated at PNPI-St. Petersburg with the help of the single-crystal diffractometer, part of the two-crystal X-ray spectrometer described in [46]. The experimental layout is as in Fig. 14. The X-ray (Mo Kα1, 17.4 keV) beam was collimated to 2 mm height and 40 μm width before incidence on the sample surface. The sample could be translated with accuracy of 1 μm and 1″ by use of a standard theodolite. A NaI counter with wide-acceptance window detected the diffracted radiation. The count rate of diffracted quanta is maximal under the Bragg condition, achieved by rotation of the sample. Below we review the results obtained in [36].

Two parameters were measured for each X-ray beam position: intensity of the diffracted beam and the angular position of the sample corresponding to a half intensity of the diffracted beam. The intensity is proportional to the integral reflectivity

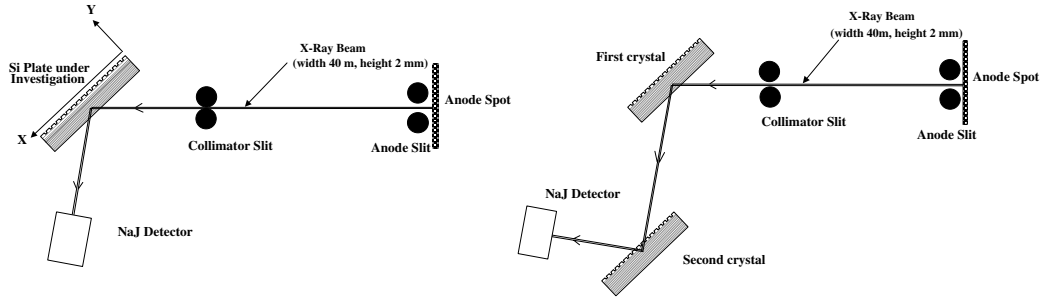


Fig. 14. Testing CU with X-rays at PNPI-St. Petersburg: one crystal (left) and two crystal (right) diffraction scheme.

of the crystal at the point of X-ray beam diffraction, and is very sensitive to crystal deformations. In the present studies, the sensitivity of this parameter to the bending of crystal planes in the diffraction area was a fraction of 1″. The angular position of the sample is related through the Bragg law to the orientation of crystal planes and to the magnitude of interplanar distance; the accuracy of angle readings was a fraction of 1″. The change in the second parameter along $x$-axis is completely due to the change in the orientation of crystal planes. The sensitivity of this parameter to the plane orientation was 2″.

Fig. 15 shows the measured intensities and angles as functions of the beam incidence position at the surface with grooves. On the same absolute scale, the position of grooves is shown as well. The periodic angular deformation of the crystal planes reach an order of 40–50 μrad. The plane deformation amplitude is in the order of 40 Å as obtained by the analysis of the angle-versus-position function.

Fig. 16 shows the corresponding values for the opposite (unscratched) face of the crystal, on the same absolute scale as in Fig. 15. One can see that the peak positions on the opposite sides match each other and match the groove positions as well; the systematic error for the absolute position in the figures is 50 μm. On the unscratched side, the local periodic deformations are smaller, just under 10 Å. If interpolated between the two faces, deformation amplitudes of order of 20 Å are expected in the bulk of the crystal. The angle of diffraction peak for X-ray diffraction in transmission mode is dis-

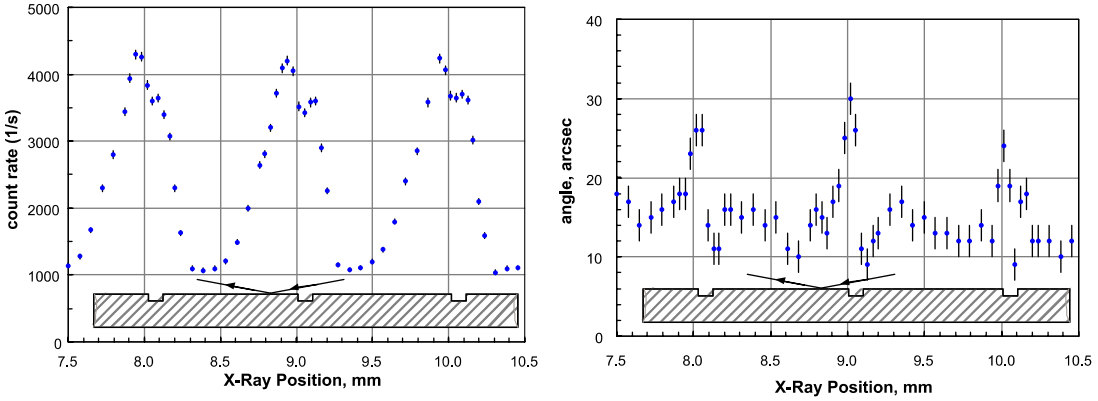


Fig. 15. Diffraction from the side with grooves: intensity (left) and angle (right) of the diffraction peak.

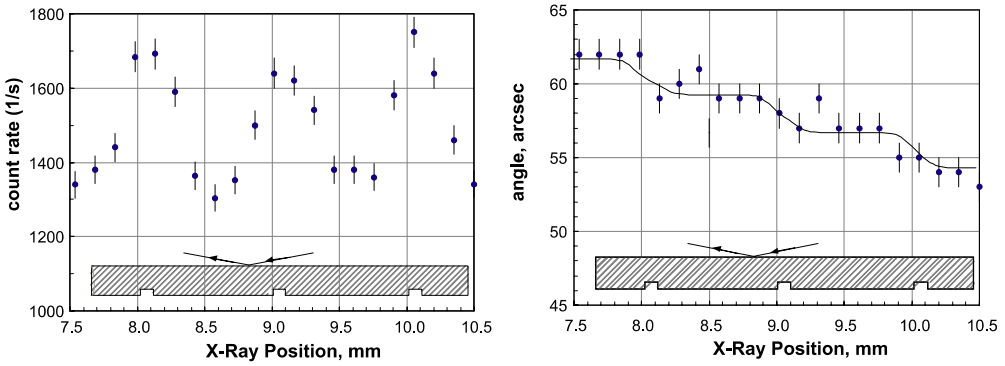


Fig. 16. Diffraction from the side without grooves: intensity (left) and angle (right) of the diffraction peak.

played in Fig. 17 for part of the sample, as well as for the whole sample. Moreover, the local deformation of the sample near the groove can be reconstructed from X-ray measurements, as shown on the left of Fig. 18. Fig. 18 (right) shows the corresponding deformation of the whole sample.

As proven by our experimental study, it is feasible to manufacture a crystalline undulator for channeling of radiating particles with a sub-millimeter period and with the amplitude of channel oscillations in the order of 20–40 Å, which is highly interesting for a novel radiation source [41,42]. Further on we have optimized the CU manufacturing process and were able to produce a series of undulators with the following parameters: the length along the beam 1–5 mm, thickness across the beam 0.3–0.5 mm, 10 periods of oscillation with period of 0.1–0.5 mm [28]. The oscillation amplitude was on the order of 50 Å. These undulators were tested with X-rays as described above. For a typical X-ray test of one of the undulators, see Fig. 19.

Based on this success, we plan two experiments on photon emission from a crystalline undulator: one at Laboratori Nazionali di Frascati with 0.5–0.8 GeV positrons, another one

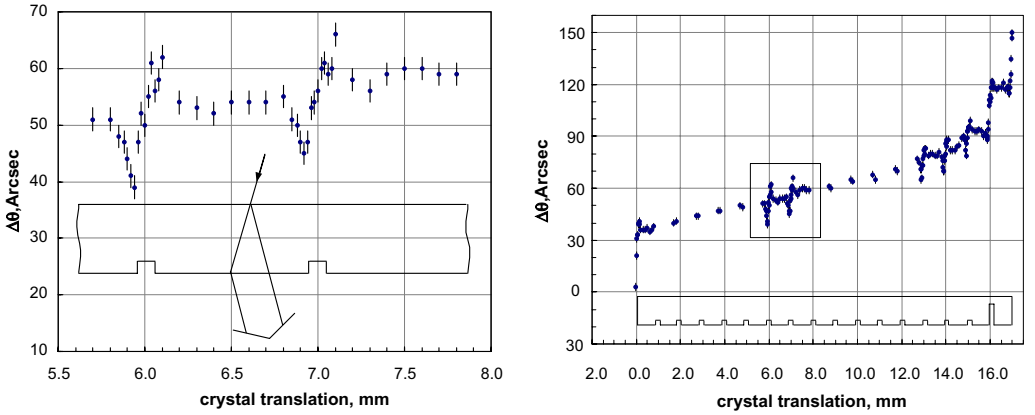


Fig. 17. X-ray diffraction in transmission mode: angle of diffraction peak for part (left) or the whole (right) of the sample.

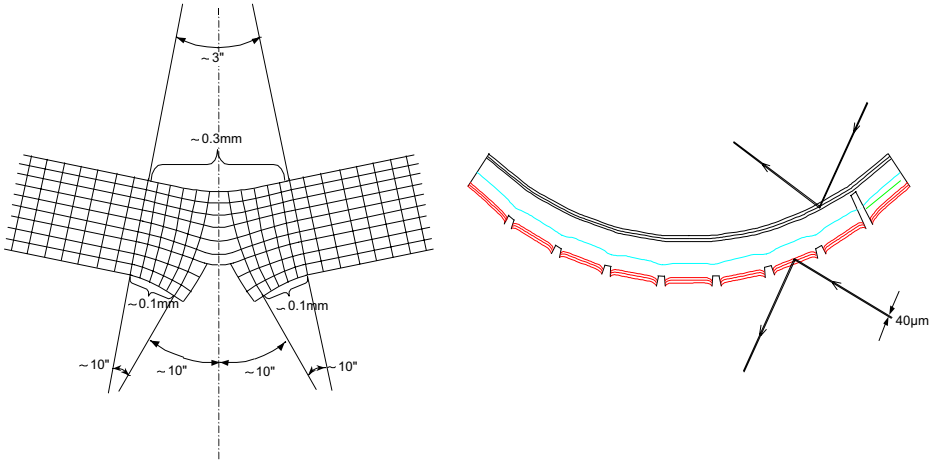


Fig. 18. Deformation of sample near groove reconstructed from X-ray measurements (left); deformation of the whole sample (right).

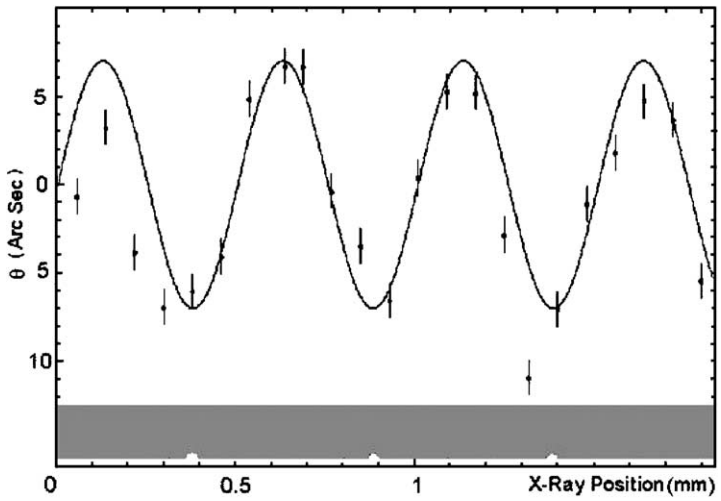


Fig. 19. X-ray test of one of the undulators.

at IHEP Protvino with 2–10 GeV positrons. For the experiments we plan to produce a grating spacing down to $L \approx 0.1$ mm to obtain CU with $\approx$10 periods (with equivalent field of $\approx$300 T). We have done preliminary simulations taking into account the following factors: (1) channeling radiation and dechanneling process; (2) finite length of the crystalline undulator; (3) radiation of the above-barrier positrons; (4) absorption of gamma-quanta in the undulator bulk. We found that a clear peak of the photon number should be observed in the range 30–60 keV at LNF. In Fig. 20 we display the expected photon spectrum at the Frascati Beam Test Facility (BTF) for 800 MeV positrons in the ranges 0–2.5 MeV (a) and 0–0.1 MeV (b). The dashed curve is the pho-

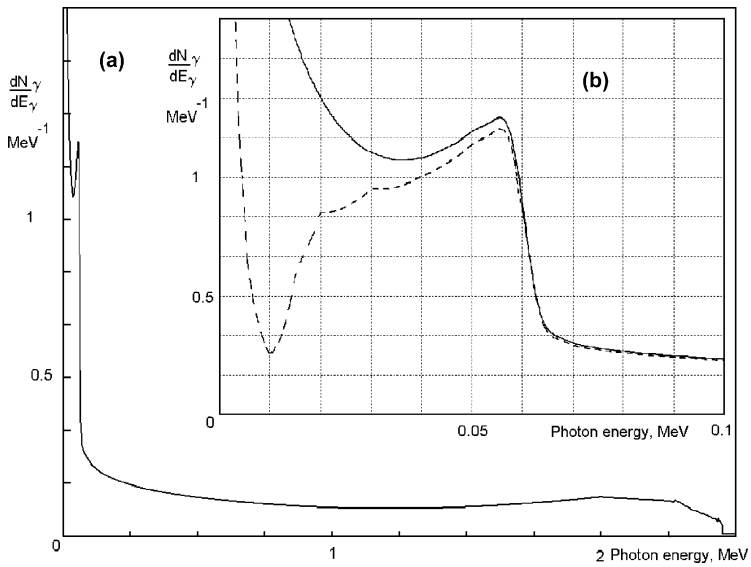


Fig. 20. Expected photon spectrum for 800 MeV positrons in the ranges 0–2.5 MeV (a) and 0–0.1 MeV (b).

ton spectrum, where the absorption process of photons in the body of undulator is taken into account. The curves are normalized on one positron passing through the undulator within the channeling angle.

In the case of IHEP we expect undulator photons in the range 100–600 keV. The spectra of undulator and channeling radiation in our crystals are well separated because of very different (two orders of magnitude) respective oscillation periods. Ref. [28] gives a very preliminary analysis of the relative importance of the above-enlisted factors (1–4) on the performance of the proposed experiments at LNF and IHEP.

The technological capabilities of the method allow us to create a CU with the full length of about 1 mm, thickness of 0.1 mm and the wavelength of $\lambda = 0.08$ mm, making $N = 10$ periods of undulator. Taking into account the positron energy of 0.5–0.8 GeV at LNF, we can obtain the following rough estimates for the characteristics of radiation in crystalline undulator.

- The undulator parameter is $K = 2\pi\gamma A/\lambda = 0.3$ (here A = 100 Å is the amplitude of undulator oscillations) in our case.
- The photon energy on the first harmonics is given by $\hbar\omega_1 = 0.95E^2\ [\mathrm{GeV}]\ L^{-1}\ [\mathrm{cm}](1+K2/^2)^{-1} = 50$ keV for 0.8 GeV positrons.
- The number of photons emitted is on the order of 0.15 per channeled positron according to our calculations [28].
- The characteristic photon emission angle is $1/\gamma = 0.6$ mrad.
- The energy spread for the radiation is about $\Delta\omega/\omega = 2/N = 0.2$.

In the experiment one can compare three different samples: (a) a straight crystal, (b) a crystal bent with a constant curvature and (c) a crystal undulator, all samples being of the same size.

The proposed experiment could be made at Frascati BTF in the external beam of positrons of maximal possible energy. The parameters of the experiment have to be optimized and more

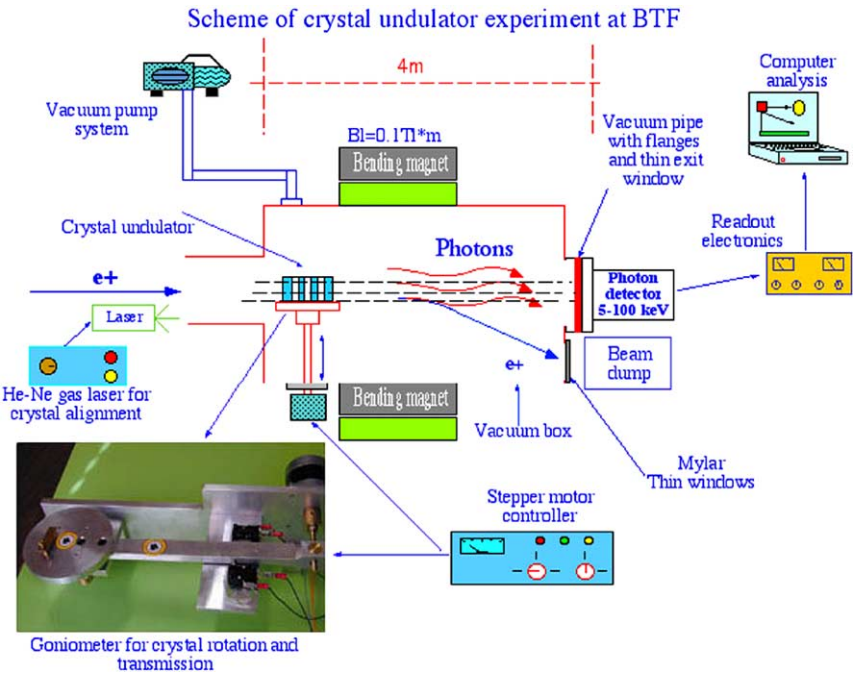


Fig. 21. The layout of the LNF experiment on photon emission in crystalline undulators.

specified in further analysis. The positron energy available at LNF is the minimum where an experiment on observation of crystalline undulator radiation is feasible. The equipment necessary to carry out the proposed experiment is outlined and explained in Fig. 21. The experiment can be run with beam intensity of $10^3$ positrons per second, with repetition rate of 25 Hz, as presently feasible at Beam Test Facility of LNF.

After the sine-like deformation of crystal was proven in X-ray tests, four undulators were tested for channeling in a beam of 70 GeV protons at IHEP. It was observed in the experiment that the crystal cross-section is efficiently channeling high-energy particles, similarly to usual crystal deflectors (see the contribution by A.G. Afonin et al., based on the talk by Yuri Chesnokov, to the present NIM B issue). The experimentally established transparency for channeling of high-energy particles allows one to start a direct experiment on photon production from a positron beam in the CU. As a completion of the future plan of activity, besides performing the first time experimental test of X-rays production by exposure of samples to positron beams (planned at LNF and IHEP with different energy ranges), we intend to prepare and study a prototype with grooves on both sides of the crystal plate.

## 5. The future of science and technology at the nanoscale in Frascati

Nanostructured materials gained great importance in the past decade, owing to their wide range of potential applications in many areas, e.g. mechanical, structural, sensor devices, biomedical, electronics. A large interest is involved with carbon nanotubes, which can be used as a main constituent of composite materials characterized by exceptional mechanical and electrical properties, very suitable for aerospace applications, due to their light weight, mechanical strength and flexibility. The synthesis and characterization of patterned films of aligned C nanotubes, comparing results obtained by different deposition methods, the optimization of the field emission properties of arc-discharge and CVD produced nanotube thin-film samples, will be continued, in order to achieve an efficient emission with high density of the emitted current, for applications to new kinds of sensor devices, e.g. pressure sensors, as well as for application to the manufacture of KV X-ray sources and gas discharge tubes based on C nanotubes.

Aluminium nitride is a wide bandgap semiconductor with very good optical and piezoelectric properties. It has very high thermal conductivity and is one of the best ceramic materials. Nanotubes of aluminium nitride have been synthesized by some of us [47], through a DC arc plasma process and characterized by various techniques. Nanotubes have many interesting applications, including those based on particle channeling through micro and nanostructures. AlN nanotubes are potential candidates for applications as gas sensors. We wish to study the process of gas adsorption, which is well characterized in the literature regarding carbon nanotubes, on AlN nanotube samples. We also wish to explore the catalytic properties of AlN nanotubes through the experimental measurement of neutron diffraction. Also it would be interesting to investigate the sensing properties of these tubes, in order to test their capabilities, e.g. as humidity and chlorine gas sensors, study the corresponding basic mechanism and quantify them with regard to their sensing properties.

The development of new low temperature and atmospheric pressure methods for the deposition of supported films of carbon nanotubes will become a main focus of activity. The same holds for the study of the reactivity of the carbon nanotubes thin films to various gas and chemical environments, as well as for the developing of methods for the functionalization of the carbon nanotubes with organic molecules and study of their reactivity to gas and chemicals, the developing of calculus models for a prediction on the functionalization and reactivity of nanotubes, the development of specific supports for the realization of organic/inorganic thin films.

An activity to synthesise metal oxide nanoparticles have recently been started by us, using an arc-discharge deposition chamber. Initially, we plan to

make nanoparticles of magnetic metal oxides, especially that of Fe, Ni and Co oxides. These may, in future, be used to dope the nanotubes (insert the nanoparticles inside the single walled or multiwalled open ended nanotubes). Such doped nanotubes can be used for biological applications. It has been reported that magnetic nanoparticles have a higher degree of magnetization and magnetic properties as compared to its bulk counterparts. The application of the produced paramagnetic nanoparticles to tumour therapy by hyperthermia is envisaged. The nanoparticles are to be coated by cell nutrients, e.g. sugar. The application of a rapidly alternating magnetic field has been proven to cause the death of the replicant cells at an effective temperature of about 45 °C.

Magnetic nanoparticles will be synthesised using thermal plasma and its properties studied vis-a-vis the bulk magnetic particles. These will then be mixed with a polymer matrix. The ratio of the polymer matrix to the magnetic particle dispersant and its effect on both mechanical as well as the residual magnetization will be studied for various matrix–dispersant ratios. The characterization techniques will include electron microscopies for confirmation and estimation of the nanoparticles prepared, X-ray diffraction for phase identification of the magnetic particles; Vibrating Sample Magnetometer, SQUID for magnetization values estimation.

In the field of mechanical properties, we will focus in particular on the study of stress sensors and analyzers based on nanostructured piezeoelectric materials, such as aluminium nitride nanotubes, that can be used for early warning of fracture development. We will also investigate the effect of reduction of fractures induced by nanotube deposition in ceramic composites. We will also measure of the electrical and mechanical properties (resilience and Young's modulus, conductivity) of a polymer matrix, reinforced with carbon nanotubes synthesized by arc discharge and other techniques, for aerospace applications. In particular, stress and numerical analysis of aerospace structures using carbon nanotubes reinforced composite materials will be carried out, together with the evaluation of the reduction weight of a typical aerospace structure.

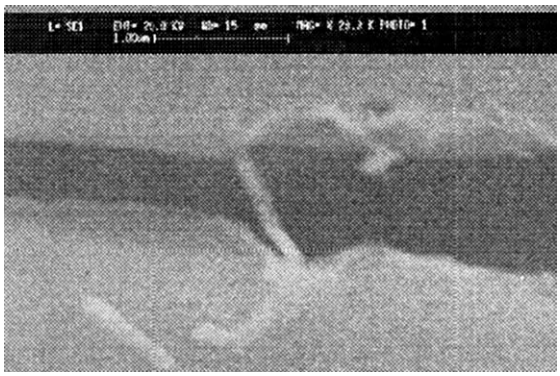

Fig. 22. SEM image of a single nanotube (AlN) resting on two gold electrodes lithographically patterned on a quartz plate.

We will work on the electrical conductivity of single, isolated nanotubes. Towards this end, we have already performed experiments to deposit individual nanotubes (of aluminium nitride) on a quartz plate with lithographically patterned gold electrodes. Fig. 22 shows a SEM image (coll. CNR-IFN) of a similar experiment carried out earlier (yet to be concluded). Similar experiments for CNTs are already in the pipeline. We will be making the lithographic patterned electrodes and studying the variation of current with voltage. The setups necessary to measure the electrical properties precisely are already present in our laboratory.

The carbon nanotubes synthesized by us could be used for the study of protein–carbon nanotube interactions for bioprobe devising. Both single walled as well as multiwalled carbon nanotubes can be studied for their suitability to these biochemical applications. The lengths of our nanotubes (up to a several microns) are in the required range (1–10 μm) for biological applications. The same applies to their straightness and stiffness. The thermal chemical vapour deposition system, which will be shortly installed, is ideal for depositing CNTs on patterned substrate which is required for studying protein–CNT interactions. The present experience (carbon based electron emitters), as well as our planned experiments on the measurement of electrical properties of single nanotubes is the ''most simple'' and basic study required for understanding the interactions of nanotube with metal proteins, Apart from the

immobilization (or controlled movement) of metal proteins on the nanotube surface, our planned study of nanotube fixation/movement on different substrates will be very useful. This, as described earlier, will be done with the help of AFM technique. The results of these experiments can be used to select an ideal substrate for CNT deposition for various purposes. The in house SEM which has been recently/renovated will be of vital help in studying the CNTs.

Irradiation of carbon NTs with energetic particles can be used for nanoengineering, e.g. for creating molecular junctions between the NTs, making NT-based quantum dots and composite materials with enhanced mechanical properties. Krasheninnikov and Nordlund [48] review ion-irradiation-induced phenomena in carbon NTs and the most promising ways of using beams of energetic particles for NT-related nanoengineering. Irradiation-induced phenomena like coalescence [49] and welding [50] of CNTs, tunneling barrier formation in CNTs by energetic Ar ions [51], creation of links between NTs [52] have been experimentally observed. Experiments also show that CNTs can be used to mask the areas below the tubes against ion bombardment [53], hence providing an alternative to the conventional electron-beam lithography in nanofabrication.

Finally, Frascati is among the proponents of a new and promising channeling activity at CERN (see the April 2004 issue of the CERN Courier, p. 33, for the general announcement and the SPSC letter by Uggeroj et al.). The studies of high-energy particle interaction with ordered matter have covered various crystal lattices (and periodic structures on micron scale, multifoils) revealing rich physics of radiation and pair production. The new structures coming, nano-ordered materials, could and should be a new target of research in the particle–solid field. The opportunity to design and engineer periodic lattices of various geometry and atomic content to fit exactly the needs and dreams of the researcher instead of choosing within natural materials, an opportunity that did not exist until recently, opens new horizons for this rich field of high-energy particle interaction with periodic structures.

## Acknowledgment

I thank all my collaborators for their help in carrying out this research and various Institutions (CNR-IFN Rome, IMM-CSIC Madrid, Univ. of Roma Tor Vergata, Univ. Pune, Univ. Modena, CNR-ISMN Bologna) for providing us with many useful images.

## References

[1] S. Iijima, Nature (London) 354 (1991) 56.
[2] S. Iijima, T. Ichihashi, Nature 363 (1993) 603.
[3] D.S. Bethune, C.H. Kiang, M.S. Devries, G. Gorman, et al., Nature 363 (1993) 605.
[4] N. Hamada, S. Sawada, A. Oshiyama, Phys. Rev. Lett. 68 (1992) 1579.
[5] Y. Saito, T. Yoshikawa, M. Okuda, N. Fujimoto, J. Phys. Chem. 54 (1993) 1849.
[6] R. Saito, M. Fujita, G. Dresselhaus, M.S. Dresselhaus, Appl. Phys. Lett. 60 (1992) 2204.
[7] K. Tanaka, K. Okahara, M. Okada, T. Yamabe, Chem. Phys. Lett. 191 (1992) 469.
[8] T.W. Ebbesen, H.J. Lezec, H. Hiura, J.W. Bennett, et al., Nature 382 (1997) 54.
[9] J.W.G. Wildoerm, L.C. Venema, A.G. Rinzler, R.E. Smalley, C. Dekker, Nature 391 (1998) 59.
[10] T.W. Odom, J.L. Huang, P. Kim, C.M. Lieber, Nature 391 (1998) 62.
[11] M.M.J. Treacy, T.W. Ebbesen, J.M. Gibson, Nature 381 (1996) 678.
[12] Y. Saito, S. Uemura, K. Hamaguchi, Jpn. J. Appl. Phys. 37 (1998) L346.
[13] H. Dai, J.H. Hafner, A.G. Rinzler, D.T. Colbert, R.E. Smalley, Nature 384 (1996) 147.
[14] C. Niu, E.K. Sichel, R. Hoch, D. Moy, H. Tennent, Appl. Phys. Lett. 70 (1997) 1480.
[15] A.C. Dillon, K.M. Jones, T.A. Bekedahl, C.H. Kang, et al., Nature 386 (1997) 377.
[16] A.G. Rinzler, J.H. Hafner, P. Nikolaev, L. Lou, S.G. Kim, D. Tomanek, P. Nordlander, D.T. Colbert, R.E. Smalley, Science 269 (1995) 1550.
[17] W.A. De Heer, A. Chatelain, D. Ugarte, Science 236 (1995) 419.
[18] P.G. Collins, A. Zettl, Appl. Phys. Lett. 69 (1996) 1969.
[19] Y. Saito, K. Hamaguchi, K. Hata, K. Uchida, et al., Nature 389 (1997) 554.
[20] J.M. Bonard, F. Maier, T. Stoeckli, A. Chatelain, W.A. De Heer, A. Kasuya, Y. Nishina, B. Jayadevan, Y. Saito, L. Forro, Ultramicroscopy 73 (1998) 7.
[21] Y. Saito, K. Hamaguchi, T. Nishino, K. Hata, K. Tohji, A. Kasuya, Y. Nishina, Jpn. J. Appl. Phys. 36 (1997) L1340.
[22] J.M. Bonard, J.P. Salvetat, T. Stoeckli, W.A. De Heer, L. Forro, A. Chatelain, Appl. Phys. Lett. 73 (1998) 918.

[23] S. Bellucci, V.M. Biryukov, Yu.A. Chesnokov, V. Guidi, W. Scandale, Nucl. Instr. and Meth. B 202 (2003) 236;
V.M. Biryukov, S. Bellucci, Phys. Lett. B 542 (2002) 111.
[24] S. Bellucci et al., in: A. Bianconi, et al. (Eds.), 19th Int. Conference on X-ray and Inner-shell Processes, American Institute of Physics, New York, 2003, p. 355.
[25] S. Bellucci, Experimental study of a crystal undulator as a new compact source of radiation, in: W. Greiner, A. Solov'yov, S. Misicu (Eds.), Proc. Symp. Channeling – Bent Crystals – Radiation Processes, 2003, p. 171.
[26] S. Bellucci, V. Biryulov, A. Cordelli, Phys. Lett. B 608 (2005) 53;
V. Biryukov, S. Bellucci, Nucl. Instru. and Meth. B 230 (2005) 619.
[27] S. Bellucci, Testing the X-rays production from crystal undulators at positron facilities, in: Proc. of the 9th Topical Seminar on Innovative Particle and Radiation Detectors on 23–26 May, 2004 in Siena, Italy, Nucl. Phys. B Proc. Suppl., in press;
V. Biryukov et al., Accelerator tests of crystal undulators, Invited talk at the NATO ARW "Advanced Photon Sources and Their Application" (Nor Hamberd, Armenia, August 29–September 02, 2004), physics/0412159;
S. Bellucci, V. Biryukov, From bent crystals to nanostructures, CERN Cour. 44 (6) (2004) 19.
[28] S. Bellucci, V.M. Biryukov, Yu.A. Chesnokov, V. Guidi, W. Scandale, Nucl. Instr. and Meth. B 202 (2003) 236;
S. Bellucci, V.M. Biryukov, Phys. Lett. B 542 (2002) 111.
[29] S. Bellucci, V.M. Biryukov, Yu.A. Chesnokov, V. Guidi, W. Scandale, Phys. Rev. Special Top. AB 6 (2003) 033502;
S. Bellucci, V.M. Biryukov, Yu.A. Chesnokov, V. Guidi, W. Scandale, Phys. Rev. Special Top. AB 7 (2004) 023501.
[30] Z. Wu, J. Zhang, K. Ibrahim, D.C. Xian, S. Bellucci, et al., Appl. Phys. Lett. 80 (2002) 2973.
[31] S. Bellucci, Phys. Stat. Sol. (c) 2 (2005) 34;
C. Balasubramanian, S. Bellucci, P. Castrucci, M. De Crescenzi, S.V. Bhoraskar, Chem. Phys. Lett. 383 (2004) 188.
[32] A. Jorio et al., New J. Phys. 5 (2003) 139.1.
[33] M.A. Pimenta, A. Marucci, S. Empedocles, M. Bawendi, et al., Phys. Rev. B 58 (1998) R16016;
S.D.M. Brown, A. Jorio, P. Corio, M.S. Dresselhaus, G. Dresselhaus, R. Saito, K. Kneipp, Phys. Rev. B 63 (2001) 155414.
[34] A.C. Ferrari, J. Robertson, Phys. Rev. B 61 (2000) 14095.
[35] J.M. Benoit, J.P. Buisson, O. Chauvet, C. Godon, S. Lefrant, Phys. Rev. B 66 (2002) 073417;
X. Zhao, Y. Ando, L.-C. Qin, H. Kataura, Y. Maniwa, R. Saito, Appl. Phys. Lett. 81 (2002) 2550.
[36] S. Bellucci et al., Phys. Rev. Lett. 90 (2003) 034801.
[37] V.V. Kaplin, S.V. Plotnikov, S.A. Vorobiev, Zh. Tekh. Fiz. 50 (1980) 1079.
[38] V.G. Barishevsky, I.Ya. Dubovskaya, A.O. Grubich, Phys. Lett. 77A (1980) 61.
[39] H. Ikezi, Y. Lin, T. Ohkawa, Phys. Rev. B 30 (1984) 1567.
[40] S.A. Bogacz, J.B. Ketersom, J. Appl. Phys. 60 (1986) 177.
[41] A.V. Korol, A.V. Solov'ov, W. Greiner, J. Phys. G: Nucl. Part. Phys. (1998) L45;
Int. J. Mod. Phys. 8 (1999) 49.
[42] R.O. Avakian, L.G. Gevorgian, K.A. Ispirian, R.K. Ispirian, Nucl. Instr. and Meth. B 173 (2001) 112.
[43] U. Mikkelsen, E. Uggerhoj, Nucl. Instr. and Meth. B 160 (2000) 435.
[44] K.A. Ispirian, private communication, in press.
[45] V.M. Biryukov, Yu.A. Chesnokov, V.I. Kotov, Crystal Channeling and Its Application at High-energy Accelerators, Springer, Berlin, 1997.
[46] S.G. Skornyakov, A.I. Smirnov, G.P. Solodov, Precision measurements of the W Lβ1, W Lβ3, Mo Lβ1, Mo Lγ1 X-ray wave lengths with two-crystal spectrometer, Preprint LNPI-1133, Leningrad, 1985.
[47] C. Balasubramanian et al., Nanotechnology 15 (2004) 370.
[48] A.V. Krasheninnikov, K. Nordlund, Nucl. Instr. and Meth. B 216 (2004) 355.
[49] M. Terrones, H. Terrones, F. Banhart, J.-C. Charlier, P.M. Ajayan, Science 288 (2000) 1226;
M. Terrones et al., Appl. Phys. A (Mater.-Sci.-Process.) 65 (2002) 355.
[50] M. Terrones, F. Banhart, N. Grobert, J.-C. Charlier, H. Terrones, P. Ajayan, Phys. Rev. Lett. 89 (2002) 075505.
[51] M. Suzuki, K. Ishibashi, K. Toratani, D. Tsuya, Y. Aoyagi, Appl. Phys. Lett. 81 (2002) 2273.
[52] H. Stahl, J. Appenzeller, R. Martel, P. Avouris, B. Lengeler, Phys. Rev. Lett. 85 (2000) 5186.
[53] W.S. Yun, J. Kim, K.H. Park, J.S. Ha, Y.J. Ko, K. Park, S.K. Kim, Y.J. Doh, H.J. Lee, J.P. Salvetat, L. Forro, J. Vac. Sci. Technol. A 18 (2000) 1329.
[54] Y. Saito, S. Uemura, Carbon 38 (2000) 169.